JOURNAL OF MATERIALS SCIENCE 35 (2000) 2949–2954

In situ measurements and analysis of imidization extent, thickness, and stress during the curing of polyimide films

H. J. KOOK
Industrial Materials Unit, LG Chemical Ltd., 20, Yoido-dong, Youngdungpo-gu, Seoul 150-721, South Korea

D. KIM*
Department of Chemical Engineering, Polymer Research Center, Sungkyunkwan University, 300, Chunchun-dong, Jangan-gu, Suwon 440-746, South Korea
E-mail: djkim@yurim.skku.ac.kr

The effects of scanning rate and pre-baking time on the imidization extent, thickness, and stress of polyimide films during the curing process were simultaneously analyzed using FTIR and the strip end deflection detector complemented with interferometer systems. Film thickness and stress increased, but imidization extent decreased with increasing scanning rates. Longer pre-baking times significantly reduced the initial film thickness and stress. Imidization extent, thickness, and stress behavior of polyimide films during the curing process were closely related one another. © *2000 Kluwer Academic Publishers*

1. Introduction

Polyimides (PIs) have good properties such as low dielectric constant, low thermal expansion coefficient, high glass transition temperature, and high mechanical strength. Because of these properties, PI films are used in a variety of interconnect and packaging applications [1–5], including passivation layers and stress buffers on integrated circuits and interlayer dielectrics in high-density interconnects on multichip modules in the electronics industry.

When PIs are used as thin films in the thickness range of some μm, they are usually coated on the substrate by a film casting method. As the initially coated PI films contain much solvent, the solvent evaporation process takes place coincidentally with the curing process. The decrease of film thickness and the variation of film properties such as thermal expansion coefficient, glass transition temperature, and mechanical properties (Young's modulus and Poisson's ratio) in both the drying and curing processes are the main causes for the generation and variation of residual stresses. As the residual stress may result in mechanical failures by delamination, cracking, and bending, its behavior should be profoundly studied for the safe application of PI films.

The stress causes the film/substrate combination to bend to maintain moment equilibrium. Founded on the bending beam theory [6], the equibiaxial stress σ_f is, to a good approximation, given by Equation 1, provided that both the thickness and Young's modulus of substrate, d_s and E_s, are much larger than those of film, d_f, and E_f, respectively,

$$\sigma_f = \frac{1}{6R} \cdot \frac{E_s d_s^2}{(1-\gamma_s)\, d_f} \tag{1}$$

Here, R is the bending curvature and γ_s the Poisson's ratio of the substrate, respectively. It is noted from Equation 1 that the determination of varying stress σ_f during the curing and drying processes is in relation mostly with both the bending curvature R and film thickness d_f, since the substrate properties such as E_s, d_s, and γ_s are almost invariant.

The stress analyses of polyimide films has been pursued by several researchers [7–12]. Their analyses, however, were based on the bending curvature measurements without *in situ* consideration of film thickness change and imidization kinetics during the curing process. In this study the stress behavior of semirigid PI, spin-coated on silicon wafer, was analyzed by *in situ* measurements of radius of curvature and thickness change using a bending beam system equipped with a laser interferometer system. The extent of imidization from poly(amic acid) (PAA) to PI during the film formation process was also determined using FT-IR. Its behavior was correlated with the stress and film thickness behavior, correspondingly.

2. Experimental

2.1. Materials

The pyromellitic dianhydride (PMDA) and oxydianiline (ODA) derived poly(amic acid) (PAA) precursor solution (PI-2545, 13.8 wt%) was supplied from

* Author to whom all correspondence should be addressed.

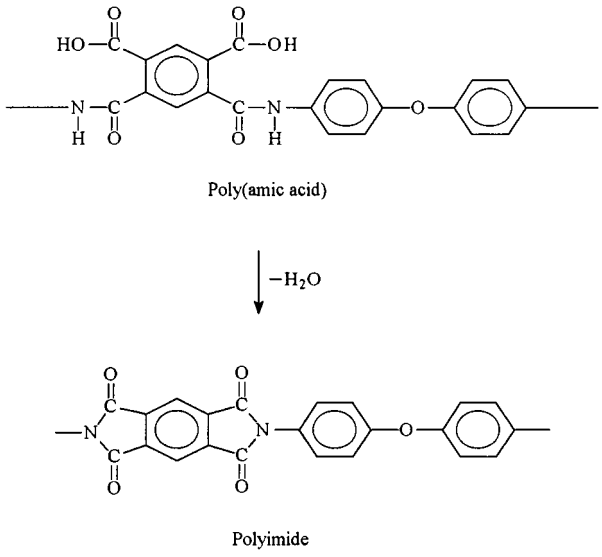

Figure 1 Synthetic mechanism of polyimide from poly(amic acid).

DuPont Chemical Company and used as received. The solvent was *N*-methyl pyrrolidone (NMP). The substrate was ⟨100⟩ type silicon (Si) wafer strip with the dimensions of 70 mm in length, 9 mm in width, and 360 μm in thickness. It was successively cleaned before use with deionized water, acetone, methanol, and HF solution. For ⟨100⟩ type Si wafer, the value of $E_s/(1-\gamma_s)$ was 1.805×10^5 MPa [13].

2.2. Film preparation

PAA solution (13.8 wt%) was spin-coated on the Si wafer substrate using the spin-coater (Model 1-EC101DT-R485, Headway research, Inc.) with the spinning speed of 1800 rpm for 30 s. After PI precursor was coated on the wafer, it was pre-baked at 80 °C for 15, 30, and 60 min, respectively, and then cured for complete imidization by heating up to 400 °C with scanning rates of 2, 4, and 6 °C/min, respectively. PAA was imidized with evaporation of solvent to the corresponding PI by the thermal imidization scheme as shown in Fig. 1. The cured film thickness was determined by measuring the weight and film dimension, and was re-examined using ellipsometer (L116B, Gaertner) and nanospec (Model 200, Nanometrics).

2.3. Film thickness and stress measurement

The stress is given by film thickness and beam curvature as expressed in Equation 1. The *in situ* measurements of film thickness and bending curvature during the PAA to PI curing process were performed using the following laser interferometer and bending beam theories.

As the solvent included in the coated film evaporated in the imidization process of poly(amic acid) to polyimide, the film thickness, d_f, in Equation 1 decreased continuously. A laser interferometer was an effective apparatus to measure this thickness change, observing the ratio of reflected to incident intensity [14–18]. In a three medium system composed of a polymer layer of refractive index n_2, air of index n_1, and a substrate of index n_3, there are two reflections, from two interfaces of polymer/air and substrate/polymer. Interference effects caused by the path difference between these two reflected light beams change the total reflection intensity. In this case, fringes were observed when the phase shift ϕ_2 changed by 2π. When the film thickness continuously changed and the incident beam angle was close to 90°, the thickness change per fringe, ΔL_2/fringe, was given by Equation 2 [15].

$$\frac{\Delta L_2}{\text{fringe}} = \left(\frac{d\phi_2/dL_2}{2\pi}\right) = \frac{\lambda}{2n_{\text{sol}}} \tag{2}$$

Here, n_{sol} is the refractive index of solvent. Thus, the film thickness change ΔL_2 during the curing process of PI was determined from Equation 2 by counting the number of fringes observed.

On the other hand, the bending curvature, R, in Equation 1 was correlated with the end deflection of film-coated substrate, δ, shown in Fig. 2 from the simple geometrical analysis.

$$R = \frac{2\delta}{l^2} \tag{3}$$

Here, l is the length of film/substrate composite strip.

Fig. 2a shows a schematic of the *in situ* measurement systems for film thickness and bending curvature. The film-coated substrate was clamped vertically in a heating block with N_2 gas purge line. Several pieces of silicon wafers were placed between the sample and clamp to inhibit transverse bending. The heating coils could raise the temperature up to 450 °C at desired scanning rates controlled by a temperature controller (Model 3000, LFE Instruments). As shown in Fig. 2b, the bending curvature measurement system was composed of a 8 mW He-Ne laser I (Model 1134P, Uniphase) as a light source, a position sensitive detector (Model 1239, UDT sensors) for the measurement of the reflected light position from the deflected strip end spot, and an oscilloscope (Model OS3040, LG Precision) for the data acquisition. The beam from laser I was focused on the top end spot of strip where the film had been specifically scratched out to minimize the interference effect. The position sensitive detector was well aligned so that the reflected laser beam position moved along the x- or y-axis of sensor. This position sensitive detector was originally designed to produce linearly increasing values of output (voltage) with increasing beam position displacement from the initially detected spot, Δ. The output from the position sensitive detector was signified by an amplifier (Model 301DIV, UDT sensors) to obtain more accurate beam displacement. After calibration of the detected laser beam intensity with its position displacement, the variation of end deflection, δ, was geometrically determined from the light position displacement, Δ, monitoring the amplified light intensity reflected from the strip end spot. No transverse bending effect on the stress was assured by observing no variation of reflected light displacement from the bare wafer strip end spot along both x and y direction of detector for similar thermal process to actual imidization process. Also, no variation of reflected light displacement was observed for the film-coated substrate along the transverse direction of the detector.

The bending curvature measurement system was complemented with an interferometer system where the

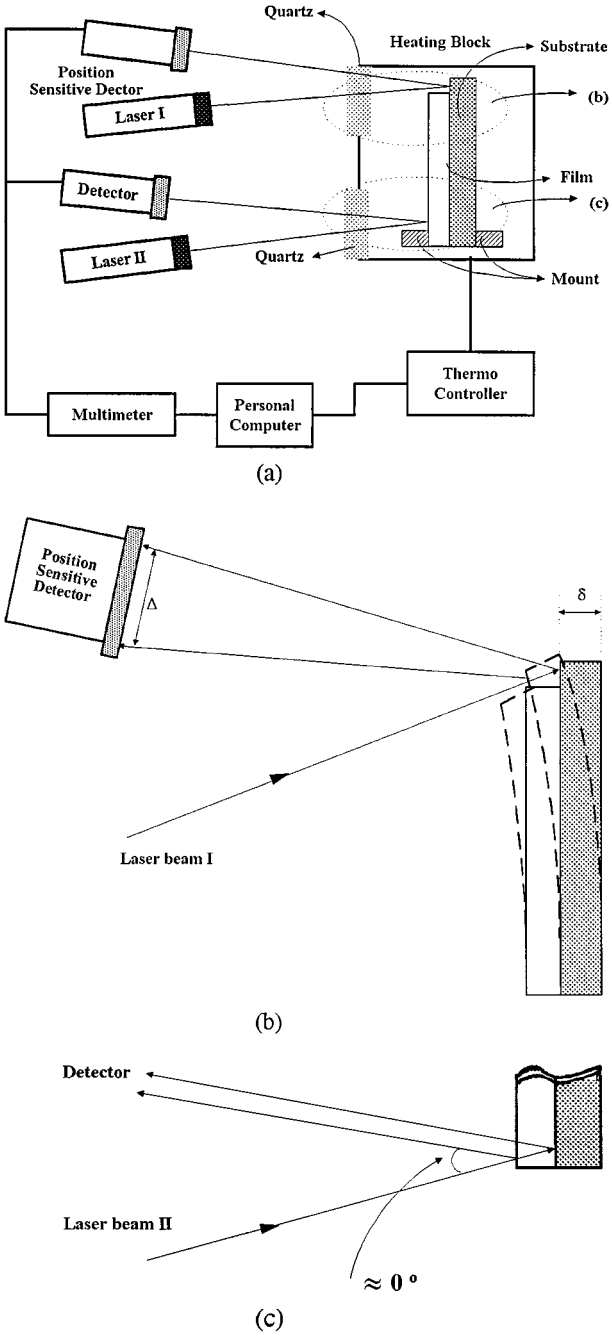

Figure 2 (a) Schematic of the *in situ* measurement systems for film thickness and bending curvature, (b) more detailed description of bending curvature measurement system, and (c) interference pattern generated at the bottom end spot of strip.

laser beam was targeted to the other end spot (bottom spot) of film/substrate strip as shown in Fig. 2a. Before measurement no bending at this very bottom spot of strip was confirmed using position sensitive detector. The interferometer system was composed of a 1mW He-Ne laser II (Model 1507P-0, Uniphase) as a light source, a photo-diode (Model S2386-8K, Hamamatsu) for the detection of reflected laser beams, and a multimeter (Model Fluke45, Fluke) for A/D conversion. As shown in Fig. 2c, the intensity of the interference signal caused by the path difference between the two reflected beams from the wafer/film and film/N_2 gas interfaces was measured by a detector.

All experiments were performed in a black box to minimize the scattering effect caused by environmental light. All optical instruments were positioned on the optical table (Edmund Scientific Company) to minimize noise. All data obtained were saved in a personal computer through a RS-232 cable.

2.4. Imidization kinetics measurement

Fourier transform-infrared (FT-IR) spectroscopy (Matison 1000, UNICAM) was used to determine the imidization extent of PAA to PI. For this experiment, PAA solution was spin-coated on Si wafer and pre-baked at 80 °C for 15, 30, and 60 min, respectively. Each film-coated wafer was broken into twelve fragments of similar size. The FT-IR spectra were obtained periodically until the completion of imidization process at each scanning rate of 2, 4, or 6 °C/min.

3. Results and discussion

3.1. Effect of scanning rate on the film thickness, imidization kinetics, and stress

After the precursor was pre-baked at 80 °C for 60 min, the variation of bending beam curvature and film thickness during the curing process was monitored *in situ* over the temperature range from 23 to 400 °C.

Fig. 3 shows the time dependence of interference signal intensity when the scanning rate was 6 °C/min. From Equation 2 the distance between the adjacent fringes corresponded to a film thickness decrease of approximately 0.216 μm, because the values of λ, the wavelength of laser and n, the refractive index of the NMP were 0.6328 μm and 1.4684, respectively. As 14 fringes were detected on heating up to 400 °C, it was noted that the total film thickness decreased by 3.024 μm for complete cure. This reduction of film thickness resulted mainly from volume reduction associated with evaporation of solvent of NMP. From the observation that the film thickness was 4.661 μm after complete cure, it was estimated that the film thickness decreased by 39% of its initial thickness during the curing process. The fact that all fringes were observed from about 200 to 350 °C revealed that the film thickness reduction was remarkable in this region.

Fig. 4 shows the FT-IR spectra of PI films during the imidization process with the scanning rate of 2 °C/min. The absorbance peak at 1776 cm^{-1} originating from the symmetric carbonyl stretching in imide group could hardly be observed at 100 °C. At temperatures above

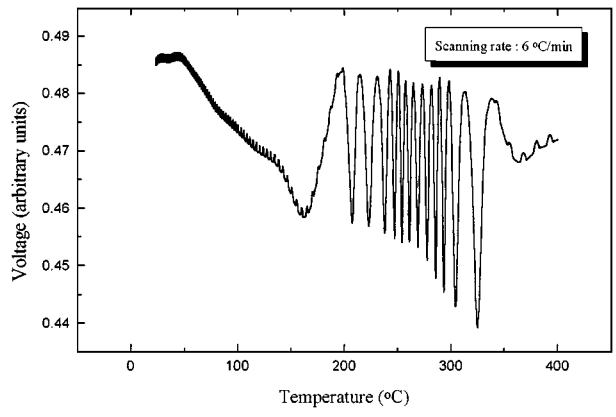

Figure 3 Voltage trace during PI curing process for the scanning rate of 6 °C/min.

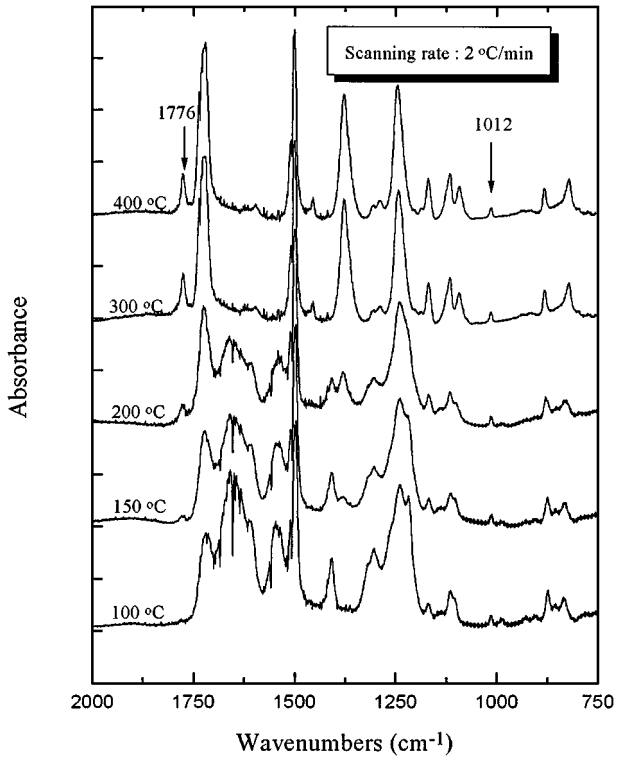

Figure 4 FT-IR spectra of PI film during the imidization process for the scanning rate of 2 °C/min.

150 °C, the peak at 1776 cm^{-1} appeared and its intensity increased with the increasing temperature. These IR spectra of PI films successively sampled during the imidization process were analyzed by the band ratio method. The area of IR peak at 1776 cm^{-1} was compared with that at 1012 cm^{-1} originating from the invariant aromatic vibration. The extent of imidization was calculated by normalizing the ratio of characteristic imide band area at 1776 cm^{-1} to the reference band area at 1012 cm^{-1} with that of the completely cured PI films. Imidization kinetics for other scanning rates of 4 and 8 °C/min were also obtained using this method.

a, b, and c of Fig. 5 show the variations of film thickness, extent of imidization, and residual stress, respectively, during the curing process of PI films for varying temperature scanning rates.

In Fig. 5a the film thickness difference, Δd_f, defined by the difference between real time film thickness and final (cured) film thickness, was represented after normalization with total film thickness difference, Δd_{f0}, defined by the difference between initial and final film thickness. The value of Δd_{f0} obtained by interferometer technique was confirmed by the measurement of initial and final film thickness using the ellipsometer. Each curve in Fig. 5a was obtained from the fringe curve as shown in Fig. 3 for the corresponding scanning rate. As the temperature scanning rates increased from 2 to 6 °C/min, the temperatures at which the variation of film thickness started and completed increased. The evaporation of solvent and water took place mostly from 23 to 280 °C with a scanning rate of 2 °C/min, from 190 to 350 °C at 4 °C/min, and from 220 to 350 °C at 6 °C/min, respectively.

The temperature dependence of imidization extent in Fig. 5b was obtained from the FT-IR spectra in Fig. 4. For the scanning rate of 2 °C/min, imidization extent

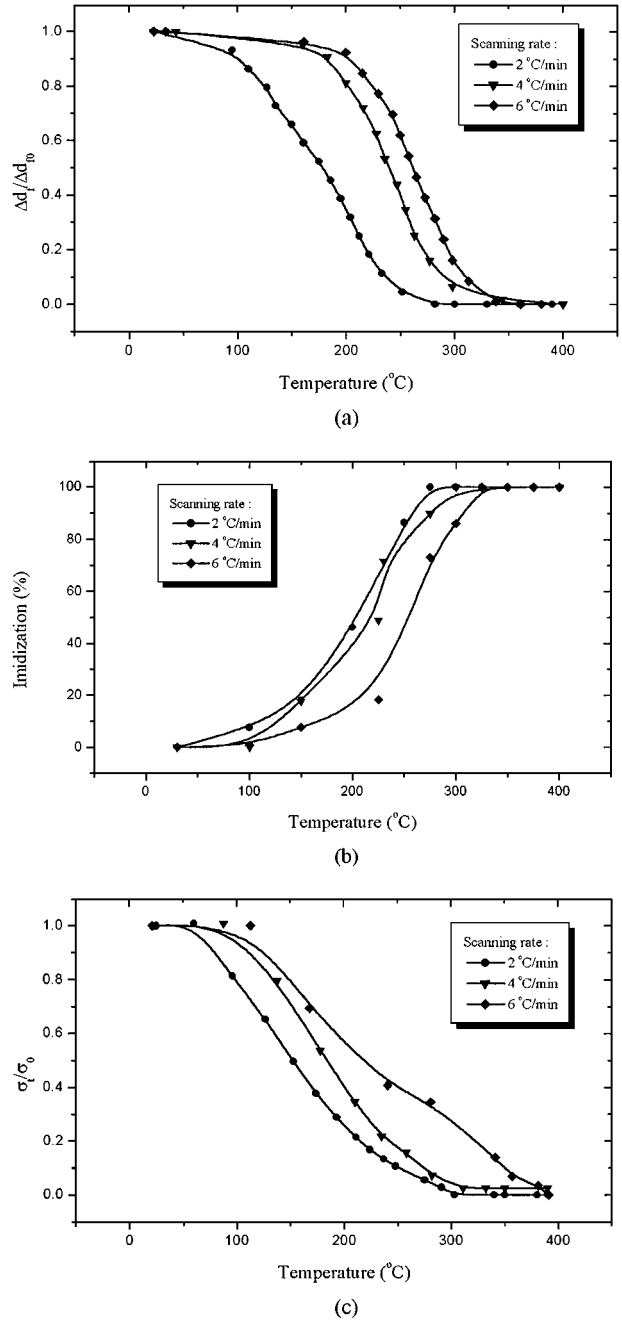

Figure 5 (a) Normalized thickness difference, (b) extent of imidization, and (c) normalized stress behavior of PI film during the curing process for the temperature scanning rates of 2, 4, and 6 °C/min, respectively; the subscripts t and 0 denote the states at arbitrary and initial curing temperatures, respectively.

was less than 10% at 100 °C, about 50% at 200 °C, and 100% at about 275 °C. The imidization process started and completed at higher temperature with increasing scanning rates. For the scanning rates of 4 and 6 °C/min, the imidization processes started from about 100 °C and completed at the temperature higher than 325 °C.

Equation 1 was possibly applied to calculate the residual stress in this system, as the maximum film thickness, d_f ($=7\sim8\,\mu$m) and Young's modulus, E_f (= about 5 GPa) of PI films during the curing processes were much lower than those of substrate, 360 μm and about 100 GPa, respectively. In Fig. 5c the stress was represented after normalization with the initial stress of $\sigma_0 = 23$ MPa. The value of stress was calculated from Equation 1 using the bending curvature and film thickness data shown in Fig. 5a. As much

solvent evaporated during the pre-baking process, the residual stress of 23 MPa was observed at the initial curing state, and then decreased to zero at complete imidization and solvent evaporation. The decreasing stress behavior was also shifted to higher temperatures with increasing scanning rates. The resulting values of residual stress were higher for higher temperature scanning rates at the fixed curing temperatures. In this imidization (thermal) process, several thermo-physical properties of polymer films such as thermal expansion coefficient, modulus and other viscoelastic relaxation properties varied continuously by the formation of network structure (imidization) and reduction of solvent. As the thermal expansion coefficient of polymer films decreased but that of substrate was almost invariant during imidization process, the decreasing thermal expansion coefficient difference between polymer films and substrate gave the most significant contributions to the increasing bending beam curvature, R, or decreasing stress in case $E_f \ll E_s$ as observed [6].

The scanning rate effect on the imidization extent, film thickness, and stress behavior was very similar in that first, temperature dependence of their behavior shifted to higher temperatures for higher scanning rates, and second, their starting and completion temperatures were almost the same.

3.2. Effect of thermal sensitivity on stress

Fig. 6a shows the sinusoidal temperature schedule applied during the curing process with the average scanning rate of 6 °C/min, and Fig. 6b shows the corresponding stress behavior. When the curing temperature oscillated, the resulting stress also oscillated significantly. This result implied that the optimal and stable control of curing schedule would be very important factors in the fabrication of PI films for safe applications.

3.3. Effect of pre-baking time on the film thickness, imidization kinetics, and stress

The variation of thickness, imidization extent, and residual stress of the PI films prebaked at 80 °C for 15, 30, and 60 min, respectively, was analyzed during the curing process.

Fig. 7a shows the prebaking time effect on the actual film thickness difference, Δd_f, in the curing process. As the pre-baking time increased, more solvent evaporated

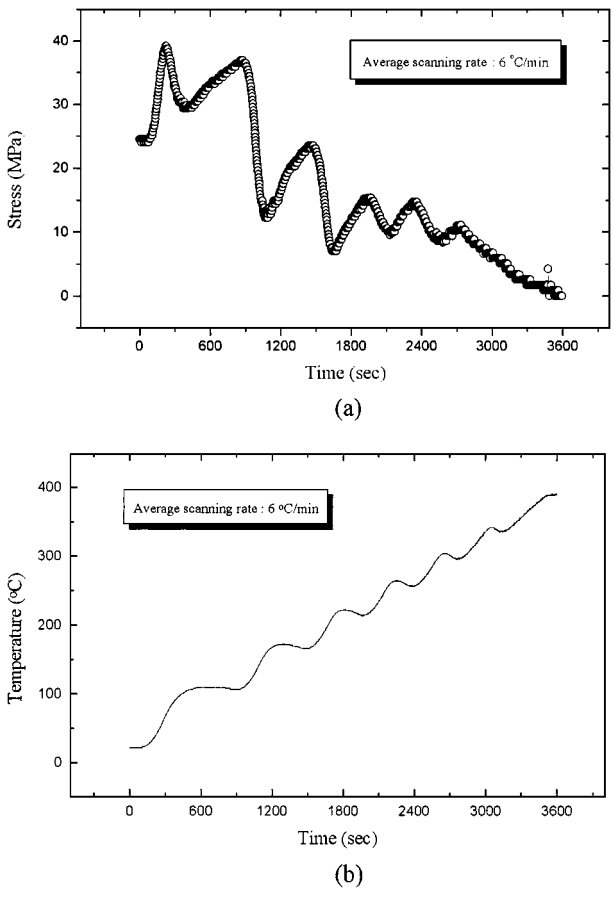

Figure 6 (a) Temperature schedule applied during the PI curing process with the average scanning rate of 6 °C/min, and (b) the resulting stress for the curing temperature schedule of (a).

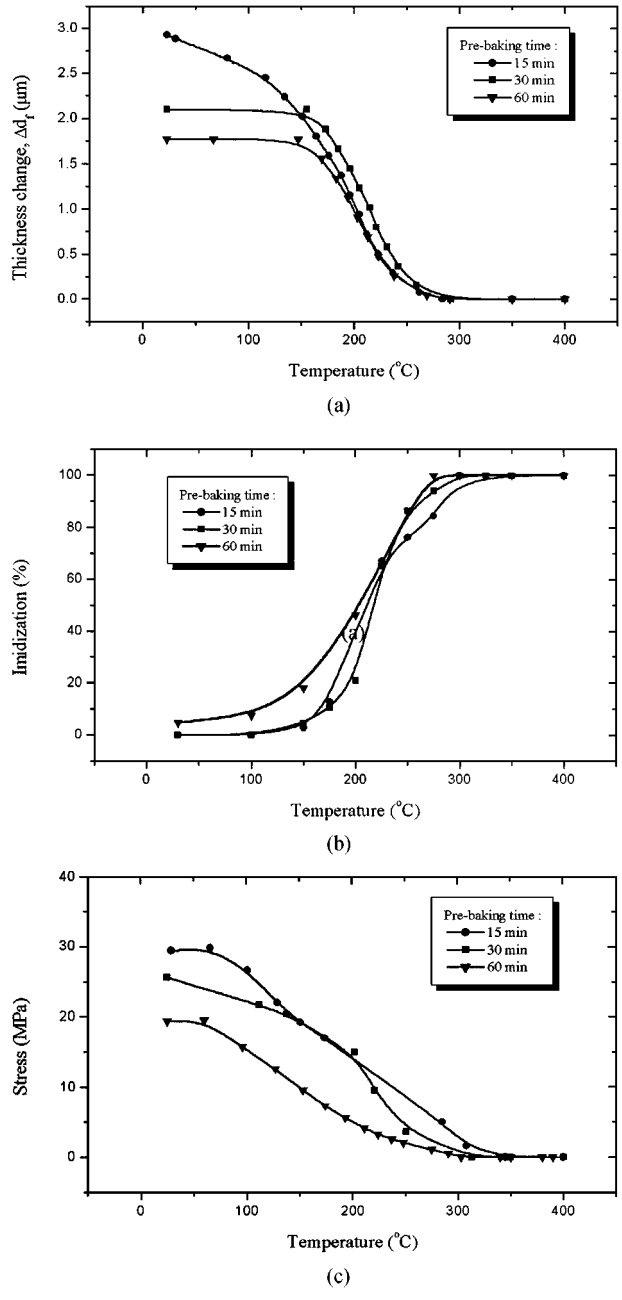

Figure 7 (a) Thickness difference, (b) extent of imidization, and (c) stress behavior during the curing process of PI films after pre-baked for 15, 30, and 60 min, respectively. The scanning rate was 2 °C/min.

during this process so that the film thickness at the end of the prebaking process decreased. By the completion of curing process after pre-baking process, the total film thickness decreased by 2.9 μm for the 15 min, 2.1 μm for 30 min, and 1.77 μm for 60 min pre-baked samples, respectively. Also, the temperature at which the film thickness started to decrease increased for the longer pre-baked samples.

Fig. 7b shows the pre-baking time effect on the extent of imidization over the curing temperature range from 23 to 400 °C. Slight imidization during the pre-baking process was observed for 60 min pre-baked samples, but not for both 15 and 30 min pre-baked samples. In the curing process, the extent of imidization for 60 min pre-baked sample was higher than 15 or 30 min pre-baked samples throughout all curing temperatures. The imidization rate was remarkable in the temperature range from 150 to 275 °C.

The effect of pre-baking times on the stress was shown in Fig. 7c with the incorporation of film thickness shown in Fig. 7a. As pre-baking time increased, the stress at the initial curing process decreased. Stress decreased to zero at around 300 °C.

4. Conclusions

The performance of cured PI films is significantly affected by the extent of imidization, residual solvent and stress in the films. Thus, the PI films fabricated even under different curing processes may provide the same performance, when the extent of curing, film thickness, and residual stress are in the same ranges. In this work the effects of temperature scanning rate and pre-baking time, major variables in the film manufacturing conditions, on the variation of the extent of imidization, film thickness, and stress in the curing process of PI films were simultaneously analyzed. Higher scanning rates resulted in the higher temperatures where the variation of imidization extent, film thickness, and stress started and completed. The decreasing trend of residual stress was sensitive in accordance with the oscillating temperature schedule. The residual stress and film thickness at the initial curing process decreased with increasing pre-baking times. Our results will provide the fundamental information of performance evaluation with respect to the operation conditions in the practical PI film fabrication.

As shown in Equation 1 the value of stress is greatly affected not only by the radius of curvature but by the film thickness, when it changes not in small amount like the present system. In this analysis the value of stress was determined by consideration of both the bending curvature and film thickness *in situ* measured during the curing process of PI films. There have been no reports in the calculation of stress with the incorporation of *in situ* measured film thickness. This is another scientific significance in this study.

Acknowledgements

This work was supported by the Korea Science and Engineering Foundation Grant 981-1109-050-2.

References

1. H. SATOU and D. MAKINO, "Polyimides for Electric Application" (Hitachi Chemical Co., Ltd., Ibaraki, 1993).
2. M. K. GHOSH and K. L. MITTAL, "Polyimides: Fundamentals and Applications" (Marcel Dekker, New York, 1996) p. 207.
3. K. SATO, K. MUKAI, S. HARADA, A. SAEKI, T. KIMURA, T. OKUBO, I. ISHI and I. SHIMIZU, *IEEE Trans on Hybrid and Packaging*, **PHP-9** (1973) 173.
4. C. C. CHAO and K. D. SCHOLZ, Proceeding of 38th Electronic Component Conference (1988) p. 276.
5. R. A. LARSEN, *IBM J. Res. Dev.* **26** (1980) 268.
6. M. OHRING, "The Materials Science of Thin Films" (Academic Press, San Diego, 1992) p. 413.
7. H. H. JOU, P. T. HUANG, H. C. CHEN and C. N. LIAO, *Polymer* **33** (1992) 967.
8. J. H. JOU and L. J. CHEN, *Macromolecules* **25** (1992) 179.
9. B. J. HAN, C. GRYTE, H. M. TONG and C. FEGER, SPE Preprint ANTEC'88 (1998) p. 994.
10. H. M. TONG, C. K. HU, C. FEGER and P. S. HO, *Polym. Eng. Sci.* **26** (1986) 1213.
11. M. REE, T. L. NUNES and G. CZORNYI, *Polymer* **33** (1992) 1228.
12. M. REE, S. SWANSON and W. VOLKSEN, *ibid*. **34** (1993) 1423.
13. F. MASEECH and S. D. SENTURIA, in "Polyimides: Materials, Chemistry and Characterization," edited by C. Feger, M. M. Khojasteh and J. E. McGrath (Elsevier, Amsterdam, 1989) p. 575.
14. B. S. KONG, Y. S. KWON and D. KIM, *Polym. J.* **29** (1997) 722.
15. K. L. SAENGER and H. M. TONG, in "New Characterization Techniques for Thin Polymer Films," edited by H. M. Tong and L. T. Nguyen (John Wiley & Sons, New York, 1990) p. 95.
16. P. D. KRASICKY, R. J. GROELE, J. A. JUBINSKY, F. RODRIGUEZ, Y. M. N. NAMASTE and S. K. OBENDORF, *Polym. Eng. Sci.* **27** (1987) 282.
17. E. HECHT, "Optics" (Addison Wesley, Massachusetts, 1987) p. 333.
18. K. L. SAENGER and H. M.TONG, *J. Appl. Polym. Sci.* **33** (1987) 1777.

Received 15 July
and accepted 6 December 1999